

Comparison of the Coil-to-Globule and the Globule-to-Coil Transitions of a Single Poly(*N*-isopropylacrylamide) Homopolymer Chain in Water

Xiaohui Wang,[†] Xingping Qiu,[†] and Chi Wu^{*,†,‡}

Department of Chemistry, The Chinese University of Hong Kong, Shatin, N.T., Hong Kong, and The Open Laboratory of Bond Selective Chemistry, Department of Chemical Physics, University of Science and Technology of China, HeFei, China

Received December 29, 1997; Revised Manuscript Received March 3, 1998

ABSTRACT: Using a newly prepared nearly monodisperse ($M_w/M_n < 1.05$) high molar mass ($M_w = 1.3 \times 10^7$ g/mol) poly(*N*-isopropylacrylamide) (PNIPAM) sample, for the first time, we successfully, for the first time, made the conformation of individual PNIPAM chains change from a coil to a fully collapsed thermodynamically stable single chain globule and then back to a coil in an extremely dilute aqueous solution ($\sim 6.7 \times 10^{-7}$ g/mL). The average chain density in the globule state is ~ 0.34 g/mL, close to 0.40 g/cm³ predicted on the basis of a space-filling model, indicating that the globule still contains $\sim 66\%$ water even in its fully collapsed state. At a given temperature around the lower critical solution temperature, the chains are smaller in the globule-to-coil transition than in the coil-to-globule transition, revealing that the coil-to-globule transition is an *irreversible* process. The hysteresis can be attributed to the formation of intrachain structures, presumably the intrachain hydrogen bonding, in the globule state. We confirmed the existence of the *crumpled* coil and the *molten* globule states between the random coil and the collapsed globule states. The coil-to-crumpled coil transition can be reasonably described by the Birshtein and Pryamitsyn theory.

Introduction

For a linear flexible polymer chain in solution, "coil" and "globule" are two distinct states, depending on the solvent quality.¹⁻¹³ The coil state in a good solvent has been repeatedly observed in various polymer/solvent systems, while the long-predicted thermodynamically stable single chain globule state in a poor solvent has not been observed. As a fundamental problem in polymer physics, the coil-to-globule transition has been extensively studied in the past 20 years¹⁴⁻²⁶ because of its application in many aspects, such as the folding of a protein chain, the packing of DNA molecules, the collapse of a polymer gel network, and the complexation between two polymer chains.²⁷⁻³⁰ However, there is only a limited experimental success despite numerous tries in different laboratories.

One of the problems in the coil-to-globule transition study is to prepare a narrowly distributed ($M_w/M_n < 1.1$) high molar mass (preferably, $\sim 10^7$ g/mol) polymer sample, which is extremely difficult, if not impossible. Polystyrene and poly(methyl methacrylate) in various organic solvents are the two mostly studied systems, because the sample preparation is relatively easy.¹⁵⁻²⁰ However, in an organic solvent, the van der Waals interaction as a driving force in the transition is so weak that each chain has no chance to reach the single chain globule state before the interchain aggregation (demixing) happens. This is why a fully collapsed thermodynamically stable single chain globule has not been really observed so far.

Using a dilute aqueous poly(*N*-isopropylacrylamide) (PNIPAM), we have studied the coil-to-globule transition since 1993, but the success is limited; namely, we observed a partially collapsed thermodynamically stable single chain globule state²⁴ but failed to reach the fully

collapsed single chain globule state. Recently, after improving the sample preparation procedure, we obtained a nearly monodisperse high molar mass PNIPAM sample in an extremely dilute solution. Using this PNIPAM solution, we have, *for the first time*, observed and studied the fully collapsed thermodynamically stable single chain globules. Moreover, reaching the thermodynamically stable globule state enabled us, *for the first time*, to study the globule-to-coil transition and compare it with the coil-to-globule transition.

Experimental Section

Sample Preparation. The synthesis of high molar mass PNIPAM was detailed before.³¹ The resultant PNIPAM was carefully fractionated by precipitation from an extremely dried acetone solution to *n*-hexane at room temperature. A fraction with a weight average molar mass (M_w) of $\sim 1 \times 10^7$ g/mol and a polydispersity index (M_w/M_n) of ~ 1.3 was obtained. With this high molar mass fraction, we first prepared a dilute aqueous solution (2.50×10^{-5} g/mL). The solution stood at room temperature for 1 week to ensure a complete dissolution. The solution was further diluted and filtered by a $0.5 \mu\text{m}$ Millipore Millex-LCR filter before laser light scattering (LLS) experiments. The combination of fractionation and filtration finally led to an extremely dilute solution (6.7×10^{-7} g/mL) containing narrowly distributed ($M_w/M_n < 1.05$) high molar mass (1.3×10^7 g/mol) PNIPAM chains. The resistivity of deionized water used was $18.3 \text{ M}\Omega \text{ cm}$.

Laser Light Scattering. In static LLS,³² we were able to obtain both the weight-average molecular mass (M_w) and the average radius of gyration ($\langle R_g \rangle$) of polymer chains in an extremely dilute solution simply from the angular dependence of the excess absolute scattering intensity, known as the Rayleigh ratio $R_{v,v}(q)$, by³³

$$\frac{KC}{R_{v,v}(q)} \cong \frac{1}{M_w} \left(1 + \frac{1}{3} \langle R_g \rangle^2 q^2 \right) \quad (1)$$

where K is a constant and $q = (4\pi n/\lambda_0) \sin(\theta/2)$ with n , λ_0 , and θ being the solvent refractive index, the wavelength of light in vacuo, and the scattering angle, respectively.

* To whom correspondence should be addressed.

[†] Chinese University of Hong Kong.

[‡] University of Science and Technology of China.

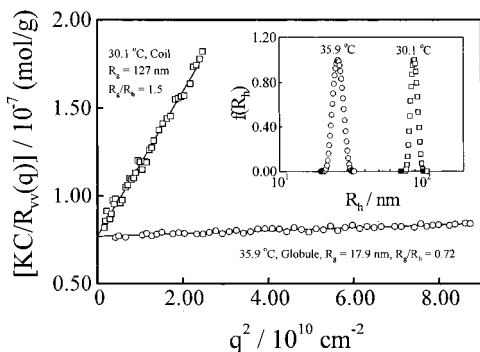


Figure 1. Typical angular dependence of $KC/R_{v}(q)$ of PNIPAM in water at two different temperatures, where the polymer concentration is 6.7×10^{-7} g/mL. The inset shows the corresponding hydrodynamic radius distributions $f(R_h)$ of the PNIPAM chains respectively in the coil and the globule states.

In dynamic LLS,^{34,35} the cumulant analysis of the measured intensity-intensity time correlation function $G^2(t)$ of narrowly dispersed polymer chains in a dilute solution is sufficient for an accurate determination of the average line width $\langle\Gamma\rangle$. For a diffusive relaxation, $\langle\Gamma\rangle$ can be further related to the average translational diffusive coefficient $\langle D\rangle$ by $\langle D\rangle = \langle\Gamma\rangle/q^2$ and the average hydrodynamic radius $\langle R_h\rangle$ by $\langle R_h\rangle = k_B T / (6\pi\eta\langle D\rangle)$ with k_B , η , and T being the Boltzmann constant, the solvent viscosity, and the absolute temperature, respectively. The hydrodynamic radius distribution $f(R_h)$ was also calculated directly from the Laplace inversion of $G^2(t)$ by using the CONTIN program.³⁶

The LLS instrumentation has been detailed before.²⁸ It should be noted that our LLS spectrometer has an unusual small angle range of $6-20^\circ$, which is vitally important for the study of the coil state of a long polymer chain because a precise determination of M_w , $\langle R_g\rangle$, and $\langle R_h\rangle$ of the polymer chains requires $q\langle R_g\rangle \ll 1$. The solution was so dilute that the extrapolation of $C \rightarrow 0$ was not necessary. The long-term temperature fluctuation inside the sample holder was less than $\pm 0.02^\circ\text{C}$.

Results and Discussion

Figure 1 shows the typical angular dependence of $KC/R_{v}(q)$ of the PNIPAM chains in the coil and the fully collapsed globule states, respectively. The decrease of $\langle R_g\rangle$ from 127 to 17.9 nm, i.e., the decrease of the slope of the lines in Figure 1 on the basis of eq 1, clearly indicates the chain collapse. The transition from the coil state to the globule state can also be directly viewed from the change of the hydrodynamic radius distribution $f(R_h)$ shown in the inset. It is worth noting that the respective extrapolations of $[KC/R_{v}(q)]_{q \rightarrow 0}$ lead to the same intercept, indicating that there is no change in M_w on the basis of eq 1, i.e., no interchain aggregation in the coil-to-globule transition. The narrowly distributed $f(R_h)$ in the globule state also indicates no interchain aggregation. Moreover, the intensity of the scattered light (I) in the globule state (not shown) is time independent, which indicates the globules are stable, because $\langle I\rangle \propto M_w \propto nM^2$ on the basis of eq 1, very sensitive to the interchain aggregation. Therefore, we are confident that what we observed is the first experimental evidence that a linear homopolymer chain is able to fully collapse into a thermodynamically stable single chain globule. Later, we will show that there also exist two other thermodynamically stable states between the coil and the fully collapsed globule states.

Figures 2 and 3, respectively, show the temperature dependence of $\langle R_g\rangle$ and $\langle R_h\rangle$ in one heating-and-cooling

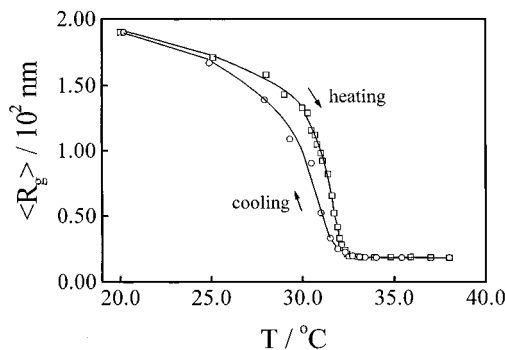


Figure 2. Temperature dependence of the average radius of gyration ($\langle R_g\rangle$) of the PNIPAM chains in the coil-to-globule (heating) and the globule-to-coil (cooling) transitions, respectively.

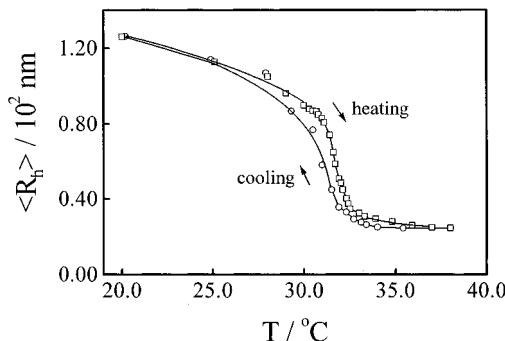


Figure 3. Temperature dependence of the average hydrodynamic radius ($\langle R_h\rangle$) of the PNIPAM chains in the coil-to-globule (heating) and the globule-to-coil (cooling) transitions, respectively.

cycle, where each data point was obtained at least 2 h after the solution reached the desired temperature even though we knew that individual PNIPAM chains can reach the equilibrium state as fast as the temperature change, typically a few hundred seconds.^{18,24} In this way, we were sure that, at each temperature, the solution was thermodynamically stable. It should be stated that the chain collapses in the heating process and the globule “melts” in the cooling process because the entropy change in the dissolution of PNIPAM is negative and the solution has a lower critical solution temperature (LCST) around $\sim 32^\circ\text{C}$. The following two points in Figures 2 and 3 are interesting: (1) in the globule state ($T > 32.3^\circ\text{C}$), the radius of gyration ($\langle R_g\rangle$) is nearly independent of the temperature in both the heating and cooling processes; (2) in the transition range $30.5-32.3^\circ\text{C}$, the PNIPAM chains in the cooling process are smaller.

It should be stated that after reaching each temperature equilibrium, no change of either $\langle R_g\rangle$ or $\langle R_h\rangle$ was observed even after the solution was kept at that temperature for 10 h. The hysteresis in the heating and cooling circle shows that the coil-to-globule transition of individual PNIPAM chains is an *irreversible* process, indicating the formation of intrachain structures, presumably the intrachain hydrogen bonding, in the globule state. It is these intrachain structures formed in the globule state that retard the “melting” of the PNIPAM globule. When the solution is cooled below $\sim 25^\circ\text{C}$, water becomes such a good solvent that all the intrachain structures are dissolved and both $\langle R_g\rangle$ and $\langle R_h\rangle$ return to their respective initial values before the heating-and-cooling cycle. Knowing $\langle R_h\rangle$, we were able to estimate the average chain density ($\langle\rho\rangle$) by using $\langle\rho\rangle$

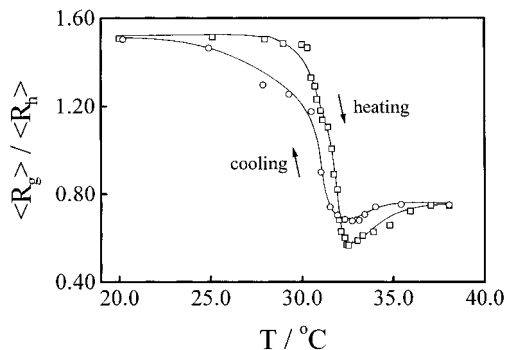


Figure 4. Temperature dependence of the ratio of radius of gyration to hydrodynamic radius ($\langle R_g \rangle / \langle R_h \rangle$) of the PNIPAM chains in the coil-to-globule (heating) and the globule-to-coil (cooling) transitions, respectively.

$\sim M_w / [N_A(4/3)\pi\langle R_h \rangle^3]$. In the coil-to-globule transition, $\langle \rho \rangle$ increases from $\sim 2.5 \times 10^{-3}$ to ~ 0.34 g/cm³, revealing that each PNIPAM globule on average still contains $\sim 66\%$ of water inside its hydrodynamic volume. It is worth noting that $\langle \rho \rangle$ obtained in this study is higher than ~ 0.2 g/cm³ previously reported for the same system²⁴ and is close to ~ 0.4 g/cm³ predicted on the basis of a space-filling model.³⁷

Another interesting point in Figure 3 is that in the heating process, $\langle R_h \rangle$ approaches a constant only when $T > \sim 37$ °C, while in the cooling process, $\langle R_h \rangle$ remains until $T < \sim 34.0$ °C, indicating that in the coil-to-globule transition, the coil gradually collapses into a uniform globule, while in the globule-to-coil transition, the swelling of the globule is relatively difficult due to the intrachain structures formed in the globule state. A comparison of Figures 2 and 3 shows that $\langle R_g \rangle$ decreases much faster than $\langle R_h \rangle$ in the temperature range 30.5–32.3 °C. It is known that $\langle R_g \rangle$ is critically dependent on the radius distribution of the chain density, whereas $\langle R_h \rangle$ is relatively more influenced by the short-range distances between atoms contiguous along the chain sequence. The difference between the coil-to-globule and globule-to-coil transitions can be better viewed in terms of $\langle R_g \rangle / \langle R_h \rangle$ because it reflects the conformation of a chain, e.g., $\langle R_g \rangle / \langle R_h \rangle$ is ~ 1.5 of a random coil chain.³⁸

Figure 4 shows that in the heating process, $\langle R_g \rangle / \langle R_h \rangle$ is nearly a constant (~ 1.50) when $T < \sim 30.6$ °C, despite the decreases of both $\langle R_g \rangle$ and $\langle R_h \rangle$ shown in Figures 2 and 3, very close to 1.504 predicted for a random coil in a good solvent and indicating no change conformation in the chain as long as the solvent is good since the Flory Θ -temperature is ~ 30.6 °C. In the temperature range 30.6–32.4 °C, $\langle R_g \rangle / \langle R_h \rangle$ decreases dramatically from 1.50 to ~ 0.56 , clearly reflecting the chain collapse in a poor solvent. In this transition temperature range, the collapsing process can be roughly divided into the two following stages: one is from 30.6 to 31.6 °C in which $\langle R_g \rangle / \langle R_h \rangle$ decreases from 1.5 to 1.0, and the other is from 31.6 to 32.4 °C. The decrease of $\langle R_g \rangle / \langle R_h \rangle$ in the first stage might reflect the conformation change from a coil to a *crumpled* coil, i.e., the formation of some blobs along the chain backbone as a chain of sausages, while in the second stage, the crumpled coil further collapses into a *molten* globule. It is worth noting that $\langle R_g \rangle / \langle R_h \rangle$ is even less than $(3/5)^{1/2}$ predicted for a uniform hard sphere.^{38,39} How could this happen? Let us examine the chain-collapsing process. It is not difficult to imagine that the collapse of a linear polymer chain leads to many small stressed loops on the surface of the globule. Hydrody-

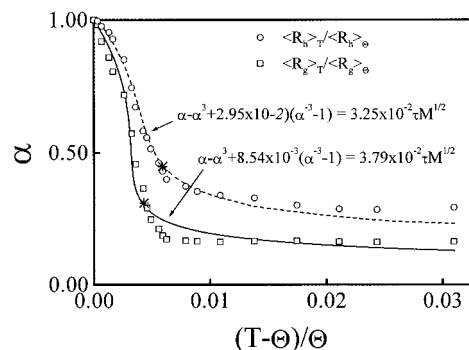


Figure 5. Temperature dependence of the contraction factor (α), where $\alpha = \langle R_g \rangle / \langle R_g \rangle_\Theta$ or $\langle R_h \rangle / \langle R_h \rangle_\Theta$. The solid and dashed lines, respectively, represent the best fitting of $\alpha - \alpha^3 + 8.54 \times 10^{-3}(\alpha^3 - 1) = 3.79 \times 10^{-2} \tau M^{1/2}$ and $\alpha - \alpha^3 + 2.95 \times 10^{-2}(\alpha^3 - 1) = 3.25 \times 10^{-2} \tau M^{1/2}$. The asterisks (*) mark the crossover from the coil state to the globule state.

namically, these loops are so small that they are not draining, which leads to a larger $\langle R_h \rangle$. On the other hand, these small loops have so small a mass that their contribution to $\langle R_g \rangle$ is negligible. This is why $\langle R_g \rangle / \langle R_h \rangle$ can be less than $(3/5)^{1/2}$. The above argument has been tested by the adsorption of polymer chains on a uniform latex particle wherein we found that $\langle R_g \rangle / \langle R_h \rangle$ is always less than $(3/5)^{1/2}$. A further increase of the temperature leads to the collapse of these small loops on the surface so that $\langle R_h \rangle$ decreases slightly, but has nearly no effect on $\langle R_g \rangle$, as shown in Figures 2 and 3. Finally, the chain collapsed into a uniform globule with $\langle R_g \rangle / \langle R_h \rangle \sim (3/5)^{1/2}$.

As shown in Figure 4, in the coil-to-globule transition (heating), $\langle R_g \rangle / \langle R_h \rangle$ reaches a lower value and the molten globule state spans a wider temperature range. Our interpretation follows. In the collapsing process, the increase of stress slows the shrinking of the small chain loops on the surface, so that the decrease of $\langle R_h \rangle$ is slower than that of $\langle R_g \rangle$; while in the melting process, there is less preference of the surface over the center of the globule in terms of the dissolution (melting) of intrachain structures formed in the globule state. A combination of Figures 2–4 shows that the decrease of $\langle R_g \rangle / \langle R_h \rangle$ at the left side of the minimum point is due to the fast decrease of $\langle R_g \rangle$, while the increase of $\langle R_g \rangle / \langle R_h \rangle$ at the right side of the minimum point is due to the decrease of $\langle R_h \rangle$. Finally, it is worth noting that the molten globule state is well-known in protein chemistry^{40–43} but has only been discovered very recently for a synthetic homopolymer that has no specific interacting sites along its chain backbone.⁴⁴

Figure 4 also shows that in the melting (cooling) process, $\langle R_g \rangle / \langle R_h \rangle$ reaches ~ 1.5 only after the temperature is lower than 25 °C, indicating that even water becomes a good solvent in the temperature range 25–30.6 °C; the globules are still not completely “molten”, or in other words, the intrachain structures formed at higher temperatures persist in the globule-to-coil process until water becomes a very good solvent. It should be noted that the globule in its molten state is nearly as compact as the globule in its fully collapsed state because there is nearly no change of $\langle R_g \rangle$ when the molten globule further collapses into the globule.

Figure 5 shows the reduced temperature ($\tau = (T - \Theta) / \Theta$) dependence of the contraction factor (α) defined as $\langle R \rangle / \langle R \rangle_\Theta$. Birshtein and Pryamitsyn suggested that α is related to τ and the molar mass (M) by⁸

$$\alpha - \alpha^3 + C(\alpha^3 - 1) = B\tau M^{1/2} \quad (2)$$

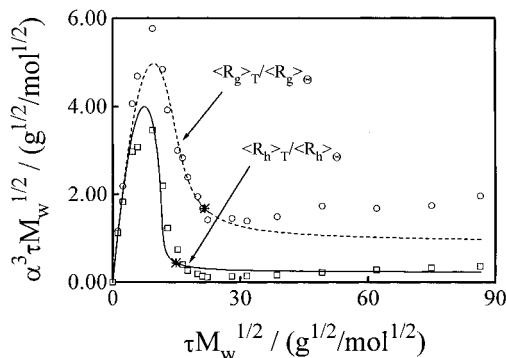


Figure 6. Plot of the scaled contraction factor $\alpha^3 \tau M_w^{1/2}$ versus $\tau M_w^{1/2}$, where $\tau = (T - \Theta) / \Theta$ and $\alpha = \langle R_g \rangle_T / \langle R_g \rangle_\Theta$ or $\langle R_h \rangle_T / \langle R_h \rangle_\Theta$. The solid and dashed lines are calculated on the basis of the best fittings in Figure 5. The asterisks (*) mark the crossover from the coil state to the globule state.

where B and C are two constants, independent of M and T for a given polymer/solvent system. In eq 2, the free energy change associated with the coil-to-globule transition contains two parts: $(\alpha - \alpha^3)$ is related to the deformation of a Gaussian chain from the unperturbed state, and $C(\alpha^{-3} - 1)$ is related to the intrachain volume interactions, depending on the total volume of the chain. The balance between these two parts, i.e., $\alpha - \alpha^3 = C(\alpha^{-3} - 1)$, is defined as the crossover point from the coil region to the globule region, which are marked by "*" in Figure 5. It is worth noting that the crossover point is far away from the Flory Θ -temperature but close to the temperature at which $\langle R_g \rangle$ approaches a constant. The solid line represents the best fitting of eq 2 with $B = 3.79 \times 10^{-2}$ and $C = 8.54 \times 10^{-3}$, and the dashed line, the best fit with $B = 3.25 \times 10^{-2}$ and $C = 2.95 \times 10^{-2}$. It can be seen that the lines fit the experimental data reasonably well in the coil region.

Figure 6 shows a plot of $\alpha^3 \tau M_w^{1/2}$ versus $\tau M_w^{1/2}$. Such a plot was reported before for polystyrene and poly-(methyl methacrylate) in various organic solvents,^{15,20} and also for PNIPAM in water.^{22,24} The theory predicts that $\alpha^3 \tau M_w^{1/2}$ should level to two asymptotic values of $C/B = 2.25 \times 10^{-1}$ and 9.08×10^{-1} , respectively, for $\langle R_g \rangle_T / \langle R_g \rangle_\Theta$ and $\langle R_h \rangle_T / \langle R_h \rangle_\Theta$. However, Figure 6 shows that after reaching the minimum, $\alpha^3 \tau M_w^{1/2}$ starts to increase as $\tau M_w^{1/2}$ increases. A combination of Figures 2, 3, and 6 reveals that the increase of $\alpha^3 \tau M_w^{1/2}$ is attributed to the increase of $\tau M_w^{1/2}$ because both $\langle R_g \rangle$ and $\langle R_h \rangle$ in the globule state are independent of the solution temperature. Our results indicate that the PNIPAM chain in an extremely dilute solution can reach its fully collapsed globule state before the demixing. All the existing theories predicted a gradual shrinking of the polymer chain until the solution enters the binodal region because they did not consider the rigidity and thickness of the polymer chain, or in other words, the chain could collapse into a finite size and the collapse stops before the demixing. In this case, the chain globule will become a "glass" ball because the local chain density in the globule is high.

On the basis of our results, both the coil-to-globule and the globule-to-coil transitions involve four distinct states: *the coil*, *the crumpled coil*, *the molten globule*, and *the globule*. The first two states can be described by the existing theories,^{1,2,4-9} but the quantitative description of the molten globule and the fully collapsed globule states remains to be a challenging problem. The

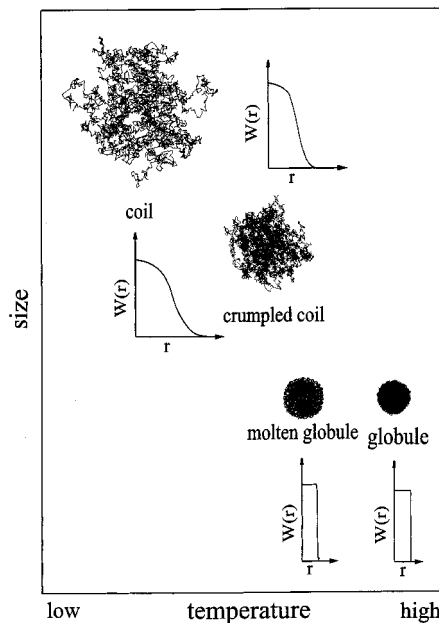


Figure 7. Schematic of four thermodynamically stable states and their corresponding chain density distributions $W(r)$ along the radius in the coil-to-globule and the globule-to-coil transitions.

deviation of the existing theories from the experimental results in the globule state is partially due to different chain density distributions, as schematically shown in Figure 7. Qualitatively, the chain collapse is related to the increase of sticking probability, which contains two parts. One is governed by thermodynamics (i.e., the effective "contact"), which increases as the solvent quality decreases; and the other is the frequency of "contact" due to Brownian fluctuations, which increases if the average distance between the segments decreases. Therefore, the collapse is a self-accelerating process. This might be one of the reasons why the transition in a real experiment is normally much sharper than the theoretical calculation.

Conclusion

We have experimentally, *for the first time*, demonstrated that a homopolymer chain can fully collapse into a thermodynamically stable globule if a narrowly distributed high molar mass polymer sample and an extremely dilute solution are used. The average chain density of the fully collapsed single chain globule is ~ 0.34 g/mL, close to ~ 0.40 g/cm³ predicted on the basis of a space-filling model, or in other words, the fully collapsed globule still contains $\sim 66\%$ water in its hydrodynamic volume. Starting from the fully collapsed single chain globule state, we were, *for the first time*, able to study the globule-to-coil transition of a single polymer chain. A comparison of the coil-to-globule and the globule-to-coil transitions reveals that there exists a hysteresis in the globule-to-coil transition and the coil-to-globule transition is an irreversible process. Our results confirmed the existence of two other thermodynamically stable states between the coil and the globule states; namely, the crumpled coil and the molten globule. The transition from the coil to the crumpled coil can be reasonably described by the existing theories, but a quantitative description of the transition from the crumpled coil to the globule state is still missing.

Acknowledgment. The financial support of the Research Grants Council of Hong Kong Government Earmarked Grant (CUHK 305/96P, 2160063) and the National Distinguished Young Investigator Fund (1996, A/C No. 29625410) are gratefully acknowledged.

References and Notes

- (1) Flory, P. J. *Principles of polymer Chemistry*; Cornell University Press: Ithaca, NY, 1953.
- (2) Stockmayer, W. H. *Macromol. Chem.* **1960**, *35*, 54.
- (3) Ptitsyn, O. B.; Kron, A. K.; Eizner, Y. Y. *J. Polym. Sci., Part C* **1968**, *16*, 3509.
- (4) Yamakawa, H. *Modern Theory of Polymer Solutions*; Harper & Row: New York; 1971. *Macromolecules* **1993**, *26*, 5061.
- (5) de Gennes, P. G. *J. Phys. Lett.* **1975**, *36*, 55.
- (6) Post, C. B.; Zimm, B. H. *Biopolymers* **1979**, *18*, 1487; **1982**, *21*, 2123.
- (7) Di Marzio, E. A. *Macromolecules* **1984**, *17*, 969.
- (8) Birshtein, T. M.; Pryamitsyn, V. A. *Macromolecules* **1991**, *24*, 1554.
- (9) Grosberg, A. Y.; Kuznetsov, D. V. *Macromolecules* **1993**, *26*, 4249 and the references therein.
- (10) Tiktopulo, E. I.; Bychkova, V. E.; Ricka, J. Ptitsyn, O. B. *Macromolecules* **1994**, *27*, 2879.
- (11) Tiktopulo, E. I.; Uversky, V. N.; Lushchik, V. B.; Klenin, S. I.; Bychkova, V. E.; Ptitsyn, O. B. *Macromolecules* **1995**, *28*, 7519.
- (12) Raos, G.; Allegra, G. *Macromolecules* **1996**, *29*, 8565.
- (13) Kramarenko, E. Y.; Khokhlov, A. R.; Yoshikawa, K. *Macromolecules* **1997**, *30*, 3383.
- (14) Sun, S. T.; Nishio, I.; Swislow, G.; Tanaka, T. *J. Chem. Phys.* **1980**, *73*, 5971.
- (15) Chu, B.; Park, I. H.; Wang, Q. W.; Wu, C. *Macromolecules* **1987**, *20*, 1965.
- (16) Yu, J.; Wang, Z. L.; Chu, B. *Macromolecules* **1992**, *25*, 1618.
- (17) Chu, B.; Yu, J.; Wang, Z. L. *Prog. Colloid Polym. Sci.* **1993**, *91*, 142.
- (18) Chu, B.; Ying, Q. C.; Grosberg, A. Y. *Macromolecules* **1995**, *28*, 180.
- (19) Dobashi, T.; Nakata, M. *J. Chem. Phys.* **1994**, *101*, 3390.
- (20) Nakata, M. *Phys. Rev. E* **1995**, *51*, 5770.
- (21) Fujishige, S.; Kubota, K.; Ando, I. *J. Phys. Chem.* **1989**, *93*, 3311.
- (22) Kubota, K.; Fujishige, S.; Ando, I. *J. Phys. Chem.* **1990**, *94*, 5154.
- (23) Meewes, M.; Ricka, J.; de Silva, M.; Nyffenegger, R.; Binkert, T. *Macromolecules* **1991**, *24*, 5811.
- (24) Wu, C.; Zhou, S. *Macromolecules* **1995**, *28*, 8381 and the references therein.
- (25) Walter, R.; Ricka, J.; Quillet, C.; Nyffenegger, R.; Binkert, T. *Macromolecules* **1996**, *29*, 4019.
- (26) Shibayama, M.; Suetoh, Y.; Nomura, S. *Macromolecules* **1996**, *29*, 6966.
- (27) Creighton, T. E. *Protein Folding*; W. H. Freeman and Co.: New York, 1992.
- (28) Chan, H. S.; Dill, K. A. *Phys. Today* **1993**, *46*, 24.
- (29) Hirokawa, Y.; Tanaka, T. *J. Chem. Phys.* **1984**, *81*, 6379.
- (30) Xiang, M.; Jiang, M.; Zhang, Y. B.; Wu, C. *Macromolecules* **1997**, *30*, 2313.
- (31) Zhou, S. Q.; Fan, S. Y.; Au-yeung, S. T. F.; Wu, C. *Polymer* **1995**, *36*, 1341.
- (32) Debye, P. *J. Phys. Colloid Chem.* **1947**, *51*, 18.
- (33) Zimm, B. H. *J. Chem. Phys.* **1948**, *16*, 1099.
- (34) Pecora, R. *Dynamic Light Scattering*; Plenum Press: New York, 1976.
- (35) Chu, B. *Laser Light Scattering*, 2nd ed.; Academic Press: New York, 1991.
- (36) Provencher, S. W. *Makromol. Chem.* **1979**, *180*, 201.
- (37) Marchetti, M.; Prager, S.; Cussler, E. L. *Macromolecules* **1990**, *23*, 3445.
- (38) Burchard, W.; Schmidt, M.; Stockmayer, W. H. *Macromolecules* **1980**, *13*, 1265.
- (39) Aksasu, A. Z.; Han, C. C. *Macromolecules* **1979**, *12*, 276.
- (40) Frauenfelder, H. *Structure and Motion: Membranes*; Plenum: New York, 1985; 7 volumes.
- (41) Ptitsyn, O. B. *J. Protein Chem.* **1987**, *6*, 273.
- (42) Martin, J. *Nature* **1991**, *352*, 36.
- (43) van der Goot, F. G. *Nature* **1991**, *354*, 408.
- (44) Wu, C.; Zhou, S. *Phys. Rev. Lett.* **1996**, *77*, 3053.

MA971873P